Temperature Dependence of TIP3P, SPC, and TIP4P Water from NPT Monte Carlo Simulations: Seeking Temperatures of Maximum Density

WILLIAM L. JORGENSEN, CORKY JENSON
Department of Chemistry, Yale University, New Haven, Connecticut 06520-8107

Received 19 June 1997; accepted 17 November 1997

ABSTRACT: Monte Carlo statistical mechanics simulations have been carried out with the TIP3P, SPC, and TIP4P models for liquid water at 13 temperatures from −50°C to 100°C at 1 atm. Long runs with 512 water molecules provided definitive results for densities. Although the TIP4P model yields a flat region in the density profile and a temperature of maximum density near −15°C, the SPC and TIP3P models show monotonically increasing density with decreasing temperature. Results for heats of vaporization, isothermal compressibilities, and coefficients of thermal expansion and their convergence characteristics are also reported. © 1998 John Wiley & Sons, Inc. J Comput Chem 19: 1179–1186, 1998

Keywords: liquid water; density; Monte Carlo simulations; water models

Introduction

The first Monte Carlo (MC) simulation of liquid water was performed by Barker and Watts[1] in 1969 and preceded the in-depth molecular dynamics (MD) studies of Rahman and Stillinger in 1971.[2] The water simulations through 1982 largely used the BNS, MCY, and ST2 potential functions and were thoroughly reviewed by Beveridge et al.[3] The TIP3P and TIP4P models[4] were introduced in 1983 and, along with the SPC model,[5] are the most commonly used water models today. In contrast to the earlier efforts, with the exception of the ST2 model,[6] their parameterization was performed in conjunction with liquid simulations and they showed improved results. The TIP3P and SPC models are similar and share a minimalist form, along with the earlier TIPS model,[7] of having just three interaction sites centered on the nuclei. Each site has a partial charge for computing the intermolecular Coulomb energy and the only additional energy term is a Lennard–Jones interaction

Dedicated to N. L. Allinger

Correspondence to: W. L. Jorgensen; e-mail: bill@adrik.chem.yale.edu

Contract/grant sponsors: National Science Foundation; Office of Naval Research

CCC 0192-8651 / 98 / 101179-08

between oxygens [eq. (1)]:

$$E_{ab} = \sum_{i}^{\in a} \sum_{j}^{\in b} q_i q_j e^2 / r_{ij} + 4\varepsilon\left[(\sigma/r_{OO})^{12} - (\sigma/r_{OO})^{6}\right] \quad (1)$$

Aside from the details of the parameters, the difference with the TIP4P model is that the site of negative charge is moved off the oxygen to a point 0.15 Å along the bisector of the HOH angle. Evaluation of an intermolecular interaction then requires computation of nine or ten intermolecular distances, and these three models use essentially the same amount of computer time. The single charge and two Lennard–Jones parameters for the models were optimized to reproduce the energy, density, and radial distribution functions for liquid water at 25°C. The ST2 model has four tetrahedrally distributed charged sites and a single Lennard–Jones interaction between oxygens[6]; it needs computation of 17 distances and requires about 35% more computer time than the three- or four-site models. Coupled with poorer performance for density, energy, and OO radial distribution function than the three simpler models for water, the ST2 model has largely been abandoned.

Because these simple models represent electrostatic interactions just with the Coulombic terms using fixed charges, they only incorporate polarization effects in an average sense. Recent developmental work on water models has focused on the explicit incorporation of polarization; however, the optimal format is still under debate.[8] The simple models will continue to receive much use and represent the key touchstone for future work. Consequently, full characterization of their properties under a wide range of conditions is important. Although this has been pursued in numerous studies, much remains to be learned. In particular, there has been great interest recently in studying the phase diagram for supercooled liquid TIP4P water including a possible liquid–liquid phase transition and the existence of a second critical point.[9] There also continues to be uncertainty about whether the simple models all yield a temperature of maximum density, the most noted of the anomalous properties of liquid water.[10] In this atmosphere, we report results of Monte Carlo simulations for the temperature dependence of the density and other properties of the SPC, TIP3P, and TIP4P models.

Computational Methods

Metropolis Monte Carlo (MC) simulations were carried out for the SPC, TIP3P, and TIP4P models in the isothermal, isobaric (NPT) ensemble at 1 atm and at temperatures every 12.5°C between −50°C and 100°C.[11] NPT-MC simulations are a particularly good choice for computing liquid densities because there is no uncertainty in the implementation of the ensemble, and the temperature and pressure controls are exact.[12] Periodic boundary conditions were used for a cubic sample of 512 water molecules with 9.0-Å spherical cutoffs based on the OO separation. The starting coordinates came from an equilibrated box of TIP4P water at 25°C; each simulation began with equilibration for 20×10^6 configurations followed initially by averaging for 40×10^6 configurations for the runs at or below 25°C and for 20×10^6 configurations above 25°C. The volume changes were attempted every 3125 configurations, and the ranges for the volume changes and the rigid translations and rotations were adjusted to yield acceptance rates of ca. 40% for new configurations. The radial distribution functions, potential energy, and volume are well converged in such long simulations.[13] Nevertheless, even greater precision for the computed volumes was sought with the TIP4P model by restarting the runs at −37.5° to 12.5°C after the initial 60×10^6 configurations and then averaging for 100×10^6 configurations. Furthermore, all results at −50°C come from equilibration for 400×10^6 configurations, followed by 400×10^6 configurations of averaging. It is expected that these are the most precise calculations that have been performed for liquid densities from water models. The density is determined from the volume by d (g cm^{-3}) = MW/(0.6022 × $\langle V(\text{Å}^3)\rangle/N$).

The heat capacity, isothermal compressibility, and coefficient of thermal expansion can be computed from the fluctuation formulas [eqs. (2)–(5)], and these converge more slowly.[13] The heat of vaporization is well approximated by eq. (6)[4b]:

$$C_p = (\partial\langle H\rangle/\partial T)_{N,P} = (1/Nk_BT^2)(\langle H^2\rangle - \langle H\rangle^2) + 3R \quad (2)$$

$$\kappa = -1/V(\partial V/\partial P)_{N,T} = (\langle V^2\rangle - \langle V\rangle^2)/k_BT\langle V\rangle \quad (3)$$

$$\alpha = 1/V(\partial V/\partial T)_{N,P} = (\langle VH\rangle - \langle V\rangle\langle H\rangle)/k_B T^2\langle V\rangle \quad (4)$$

$$H = E(\text{liq.}) + PV = \sum_{a<b} E_{ab} + PV \quad (5)$$

$$\Delta H_{vap} = E(\text{gas}) - E(\text{liq.}) + P(V(\text{gas}) - V(\text{liq.})) \approx -\langle E(\text{liq.})\rangle/N + RT \quad (6)$$

Thermodynamic Results at 25°C

Some properties of liquid water computed with the SPC, TIP3P, and TIP4P models at 25°C are compared with experimental data in Table 1. Although C_p and κ were computed from the fluctuations formulas, the values reported for α came from the computed volumes at 12.5° to 37.5°C. The indicated statistical uncertainties are 1σ and were obtained from the fluctuations in averages for batches of 5×10^5 configurations. The results are very close to the original findings obtained from shorter simulations, for instance, for a system with 216 TIP4P water molecules with an 8.5-Å cutoff, and averaging for 3×10^6 configurations, the density and ΔH_{vap} were found to be 1.002 g cm^{-3} and 10.70 kcal/mol.[4]

Most properties of the simple water models are in good agreement with the experimental values. The dielectric constant is difficult to compute and requires long simulations; for TIP4P water, values of 53, 61, 72, and ca. 50 have been reported.[15a, 16–18] The dielectric constant for SPC water at 25°C has been computed to be 54, 68, and 72[15, 16]; similar values can be expected for TIP3P water in view of the similarity of the models; for example, the charge on oxygen is −0.820 with SPC and −0.834 with TIP3P. However, in molecular dynamics calculations, the three-site models give a diffusion constant that is too high ($4–5 \times 10^{-5}$ cm^2/s),[19] whereas this property is improved in comparison to the experimental value (2.4×10^{-5} cm^2/s) with the TIP4P model (2.8×10^{-5} cm^2/s).[18] The TIP4P model is robust; prior MC simulations over a 125° temperature range at 1 atm and from 1 atm to 10,000 atm at 25°C reveal average errors of less than 2% for the computed densities.[4b, 20]

Water Structure at 25°C

As shown in Figure 1, another strong point for the TIP4P model is the OO radial distribution function, which has clear second and third peaks near 4.5 and 6.8 Å in accord with experiment.[21] In comparison, the three-site models have more difficulty yielding structure beyond the first peak in the OO rdf.[4, 5] The SPC model yields a small second peak in NPT simulations, although it largely disappears when the density is raised to the experimental value.[4a] The three models all yield good

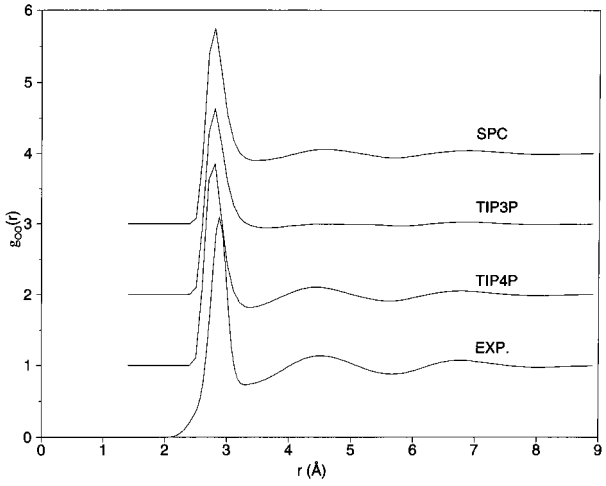

FIGURE 1. Computed and experimental oxygen–oxygen radial distribution functions for liquid water at 25°C and 1 atm. Successive curves are offset 1 unit along the ordinate.

TABLE I.
Computed and Experimental Thermodynamic Properties of Water.[a]

Property	SPC	TIP3P	TIP4P	Exp.[b]
d (g cm^{-3})	0.985 ± 0.001	1.002 ± 0.001	1.001 ± 0.001	0.997
ΔH_{vap} (kcal/mol)	10.74 ± 0.01	10.41 ± 0.01	10.65 ± 0.01	10.51
C_p (cal/mol K)	20.2 ± 0.6	20.0 ± 0.6	20.4 ± 0.7	18.0
$10^6\ \kappa$ (atm^{-1})	60 ± 4	64 ± 5	60 ± 5	45.8
$10^5\ \alpha$ (deg.$^{-1}$)	106 ± 8	144 ± 8	44 ± 8	25.7
ε	54, 68, 72[c]		53, 61, 72[d]	78

[a]Results at 25°C and 1 atm. [b]Refs. 4, 14. [c] Results from refs. 15, 16. [d]Results from refs. 16–18.

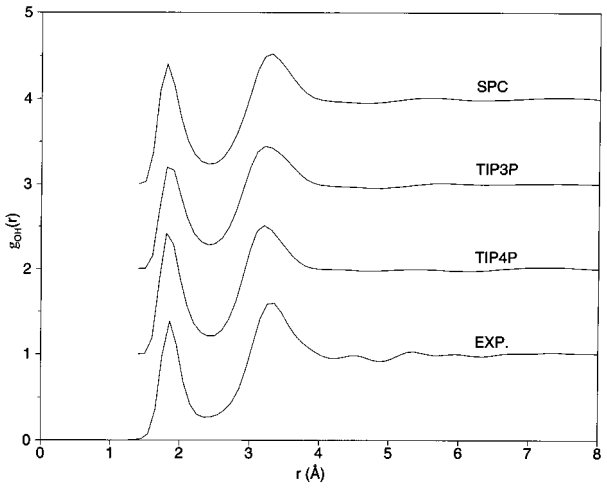

FIGURE 2. Computed and experimental oxygen – hydrogen radial distribution functions for liquid water at 25°C and 1 atm. Successive curves are offset 1 unit along the ordinate.

accord with the experimental OH and HH rdfs in Figures 2 and 3. The hydrogen bonding in liquid water has been thoroughly characterized in numerous simulation studies.[2–4,6,20] At 25°C and 1 atm, about 50% of the monomers participate in four hydrogen bonds with ca. 8%, 33%, and 10% in two, three, and five hydrogen bonds for an average of 3.6 hydrogen bonds per monomer. The first peak in the OH rdf best reflects the hydrogen bonding; its integral to 2.5 Å gives an average of 3.9 hydrogen bonds per monomer. The coordination number from integration of the first peak in the OO rdf out to 3.5 Å is 5.0 from experiment and the calculations, so the first peak contains more than hydrogen-bonded neighbors.

The OO rdf and diffusion constant are improved in a three-site format by increasing the magnitude of the partial charges as in the SPC/E model.[19] This also decreases the energy of the liquid; however, it was argued that this was justified to compensate for the cost of the enhanced polarization of the water molecules in the effective pair potentials.[19a] The dipole moment for a water molecule in the three- and four-site models is ca. 2.2 D vs. the experimental 1.85 D for an isolated water molecule. This polarization correction is not well defined and may exceed the limits of physical significance attachable to the models. For example, the dipole moments of the models are computed from the point-charges, whereas the experimental value is from the full electron-density distribution. Furthermore, one could add other $1/r^n$ terms to such potential functions and use smaller charges, which would arbitrarily change the ''polarization correction.''

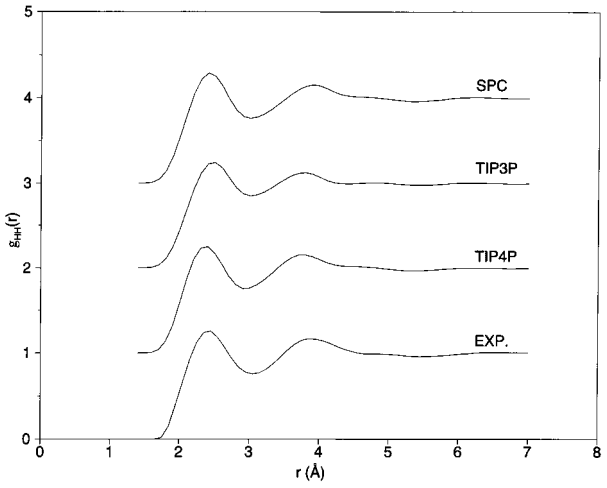

FIGURE 3. Computed and experimental hydrogen – hydrogen radial distribution functions for liquid water at 25°C and 1 atm. Successive curves are offset 1 unit along the ordinate.

Temperature Dependence of Thermodynamic Properties

The computed results for the density, ΔH_{vap}, C_p, κ, and α are compared with the experimental data[14] in Figures 4–8. The fluctuation formulas, eqs. (2)–(4), were only used to provide the data for κ in these plots; κ could not be computed by differentiation because the pressure was not var-

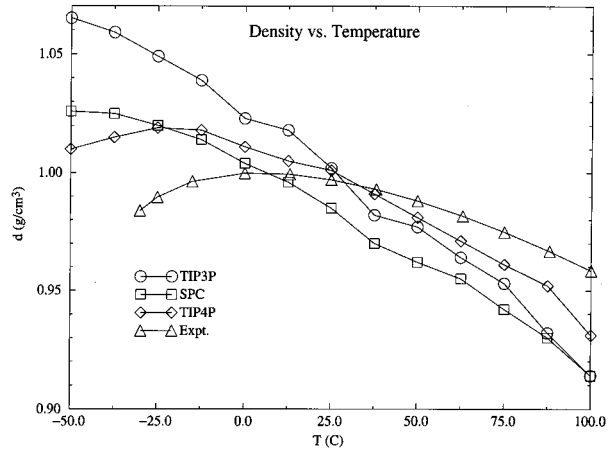

FIGURE 4. Computed and experimental densities for liquid water.

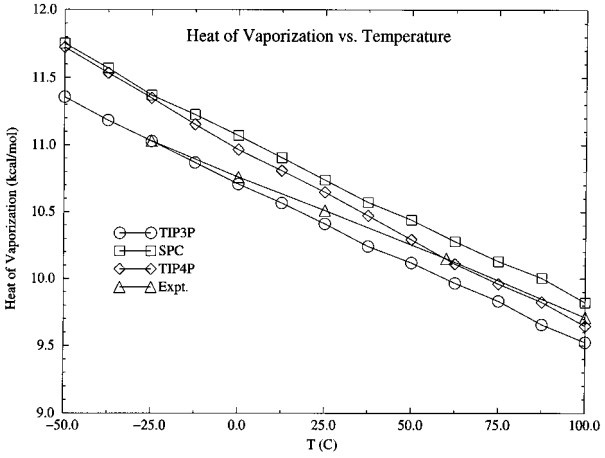

FIGURE 5. Computed [eq. (6)] and experimental heats of vaporization for liquid water.

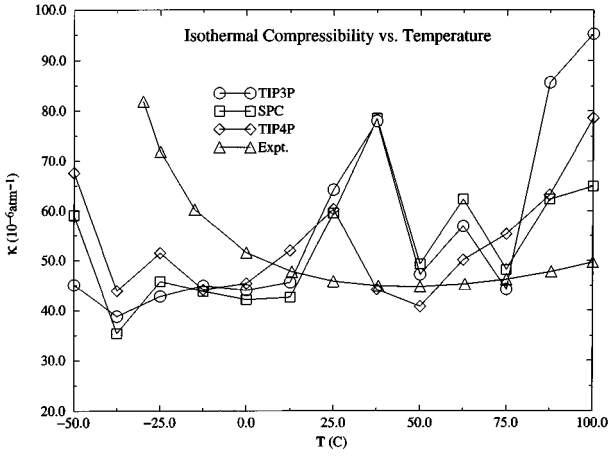

FIGURE 7. Computed [eq. (3)] and experimental isothermal compressibilities for liquid water.

ied. For C_p and α, the plotted results are from taking the numerical temperature derivative for the enthalpy and volume for the two temperatures on either side of the data point; for instance, at 12.5°C and 37.5°C for the results at 25°C. The resultant curves for the computed quantities vs. temperature are significantly smoother than from plotting the results from the fluctuation formulas. Even so, the relative smoothness of the computed curves for the density and ΔH_{vap} clearly reflects their faster convergence than for the fluctuation properties.

DENSITY

The densities are also provided in Table II from the longest runs in each case. Additional information on their convergence is provided in Figure 9, which contains the averages for every batch of 5×10^5 configurations and the running average for the TIP4P results at $-25°$, $-12.5°$, and 0°C from averaging for the original 40×10^6 configurations. The running averages change by less than 0.005 g cm^{-3} after ca. 15×10^6 configurations. It may also be noted that, in 1985, results were reported for TIP4P water at 1 atm from MC simulations with 216 molecules and 8.5-Å cutoffs at $-25°$,

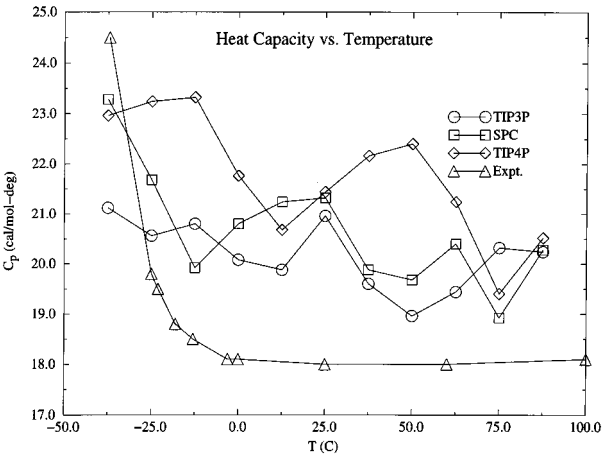

FIGURE 6. Computed (by differentiation) and experimental heat capacities for liquid water.

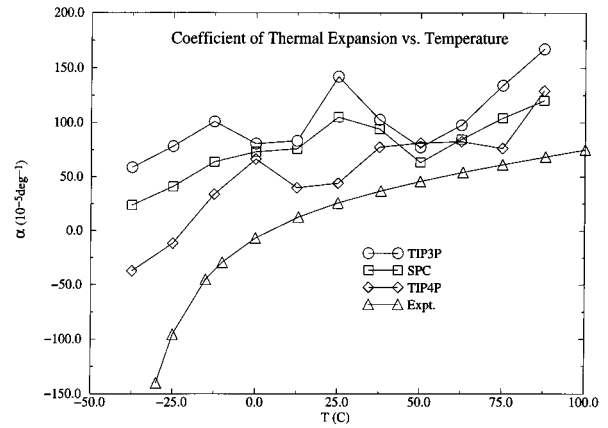

FIGURE 8. Computed (by differentiation) and experimental coefficients of thermal expansion for liquid water.

TABLE II.
Computed and Experimental Densities of Liquid Water (g cm^{-3}).[a]

Temp. (°C)	SPC	TIP3P	TIP4P	Exp.[a]
−50.0	1.026	1.065	1.010	
−37.5	1.025	1.059	1.015	(0.9752)[b]
−25.0	1.020	1.049	1.019	0.9896
−12.5	1.014	1.039	1.018	0.9972
0.0	1.004	1.023	1.011	0.9998
12.5	0.996	1.018	1.005	0.9994
25.0	0.985	1.002	1.001	0.9970
37.5	0.970	0.982	0.991	0.9931
50.0	0.962	0.977	0.981	0.9880
62.5	0.955	0.964	0.971	0.9819
75.0	0.942	0.953	0.961	0.9748
87.5	0.930	0.932	0.952	0.9670
100.0	0.914	0.914	0.931	0.9584

[a]Ref. 14a.
[b]Extrapolated.

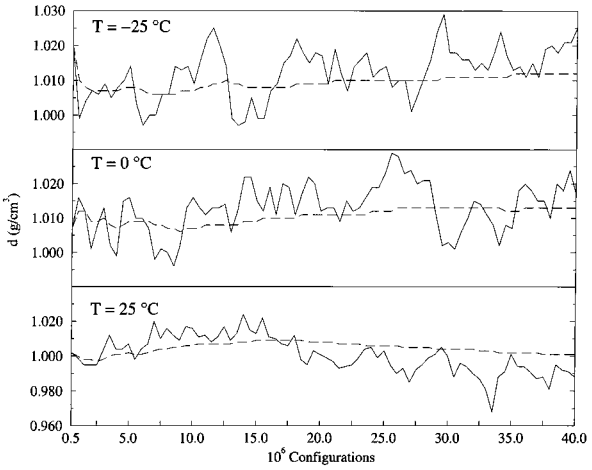

FIGURE 9. Separate averages (solid line) for blocks of 5×10^5 configurations and the running average (dashed line) of the density of liquid TIP4P water computed with Monte Carlo simulations at −25°, −12.5°, and 0°C.

0°, 25°, and 100°C; the densities were 1.008, 1.020, 1.002, and 0.929 g cm^{-3}.[4b] These differ from the new results by 0.011, 0.009, 0.001, and 0.002 g cm^{-3}. The averaging runs of 3×10^6 configurations in that study were too short at the lower temperatures. Presently, the average difference for the densities of TIP4P water from the additional 100×10^6 configurations of averaging vs. the original 40×10^6 configurations for the five data points at −37.5° to 12.5°C is 0.003 g cm^{-3}. These results coupled with the apparent residual noise in the curves in Figure 4 indicate that the computed densities are precise to this level.

Experimentally, the temperature of maximum density is not a sharp phenomenon. As shown in Figure 4, the principal feature is that the experimental density is essentially constant from −15° to +15°C. This behavior is also found in the TIP4P results, although shifted to the −35° to 0°C range and with the maximum occurring around −15°C rather than at the experimental 4°C. Series of molecular dynamics (MD) simulations at both constant pressure and temperature have also located a temperature of maximum density for TIP4P water near 260 K (−13°C) at P = 1 atm; the densities reported by Stanley and coworkers at −50° to 25°C are identical to the present results,[9a,b] whereas those of Tanaka are uniformly higher by 0.01−0.02 g cm^{-3}.[9c,d] It may be noted that the MD studies used periodic cells with 216 TIP4P water molecules as compared with the 512 molecules used here; thus, the density results show insignificant dependence on system size, as previously found.[4b]

In contrast, the SPC and TIP3P models yield monotonically increasing density with decreasing temperature; the results in Figure 4 are nearly linear with average α's of 90×10^{-5} for SPC and 110×10^{-5} deg.$^{-1}$ for TIP3P. The experimental density curve is comparatively flat. The density ranges for the −38° to 100°C region from the three-site models, 0.11 for SPC and 0.15 for TIP3P, are substantially larger than the experimental value of 0.04 g cm^{-3}, whereas the 0.09 g cm^{-3} range with TIP4P shows some improvement. The average error for the densities between 0 C and 50 C is only 0.006 g cm^{-3} with TIP4P, whereas it is 0.014 g cm^{-3} with both the SPC and TIP3P models.

The reason for the better density results with TIP4P is undoubtedly associated with the fact that the optimal water dimer structure is more bent with a flap angle, τ, of 46° with TIP4P vs. 21° for SPC and TIP3P. This promotes a more tetrahedral network in

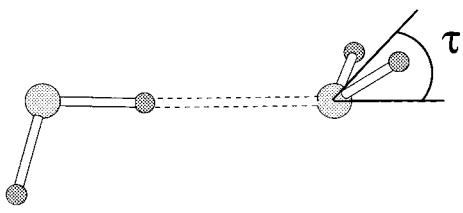

the liquid, which is also reflected in the significant second peak in the TIP4P oxygen–oxygen rdf (Fig. 1). For reference the optimal dimerization energies are −6.61, −6.54, and −6.23 kcal/mol for SPC, TIP3P, and TIP4P, respectively, and the optimal OO distance is 2.75–2.76 Å in each case. It is notable that the model with the weakest dimer interaction gives the better liquid structure and properties. The ST2 model is even more tetrahedral with $\tau = 52°$, has a stiffer potential for bending τ than the three- and four-site models, and has a more bound optimal dimer, −6.84 kcal/mol.[4a] It yields an overly structured oxygen–oxygen rdf.[4a] Although it exhibits a temperature of maximum density, it is at too-high temperature by 35° (ca. 40°C for P = 1 atm).[22]

It should be noted that the present results for SPC water are consistent with the MD investigation by Billeter et al., which did not show a temperature of maximum density for either SPC or SPC/E water in the −15° to 25°C range.[10a] Báez and Clancy reported a temperature of maximum density for SPC/E water at −38°C from NPT-MD simulations.[10b] The SPC model may also yield a temperature of maximum density near this point in view of the essentially identical densities obtained here at −37.5° and −50°C (Table II). At the other extreme, there have also been studies of the performance of the simple water models in the supercritical regime at temperatures above 400°C and at pressures of 1 to 1000 atm, which is far outside their realm of parameterization.[23] The trend toward underestimation of the density with increasing temperature remains and the critical temperature from the SPC and TIP4P models appears to be too low by ca. 50°.

OTHER PROPERTIES

In Figure 5, the computed heats of vaporization are shown to vary nearly linearly with the temperature over the 150° range. This is consistent with the essentially constant, experimental heat capacity from 0°C to 100°C. From the computed enthalpies at 12.5° to 37.5°C, and adding 3R for the kinetic term, the heat capacities are all 20 to 21 cal/mol K for the SPC, TIP3P, and TIP4P models (Fig. 6). Although these values agree well with the results of 20 cal/mol K computed with the fluctuation formula at 25°C (Table I), plots of the fluctuation results indicate uncertainties of 1 to 2 cal/mol K above 0°C and ca. 5 cal/mol K at lower temperatures. The results from the numerical differentiation in Figure 6 are better behaved, but still suggest uncertainties of ca. 1 to 2 cal/mol K. A striking anomaly of water is the rapid increase in C_p in the supercooled regime.[14c] The trend is apparent in the computed results, although the noise in Figure 6 is substantial.

The results for the isothermal compressibility and coefficient of thermal expansion in Figures 7 and 8 also show significant statistical noise. The anomalous experimental minimum in κ at 46°C is much too subtle for detection with the present NPT simulations. However, the computed α's clearly reveal the observed trend toward increasing values with increasing temperature. Furthermore, the TIP4P predictions are closer to the experimental curve, as expected from the density results, and the computed negative α with TIP4P at −25° and −37.5°C reflects the existence of the temperature of maximum density. The only negative results from use of the fluctuation formula for α are for TIP4P water at −37.5° and −50°C and for SPC water at −50°C with values of -98×10^{-5}, -22×10^{-5}, and -8×10^{-5} atm^{-1}.

Conclusions

The present study has provided fundamental results on the temperature dependence for properties of liquid water with the widely used SPC, TIP3P, and TIP4P models. Although all three models are viable in many contexts, the TIP4P model consistently yields better accord with experimental thermodynamic and structural data than the three-site models. A principal focus here has been confirmation that the TIP4P model does find a flat region in the density profile and a temperature of maximum density near −15°C, whereas the three-site models show monotonically increasing density with decreasing temperature. The better performance in all areas with TIP4P is associated with its more bent description of the water dimer. There is still room for improvement in the computed density vs. temperature profile, which probably requires a model that yields an even more bent dimer, on average. The present results also further illustrate that the radial distribution functions, heats of vaporization, and densities can be obtained readily with high precision from NPT Monte Carlo simulations. However, with the use of the fluctuation formulas, convergence of heat capacities to better than 1 cal/mol K is difficult and only semiquantitative results can be obtained for the isothermal compressibility and coefficient of ther-

mal expansion; direct differentiation of results from NPT simulations at multiple temperatures and pressures is numerically preferred.

Acknowledgment

The authors thank Dr. Julian Tirado-Rives for assistance.

References

1. J. A. Barker and R. O. Watts, *Chem. Phys. Lett.*, **3**, 144 (1969).
2. A. Rahman and F. H. Stillinger, *J. Chem. Phys.*, **55**, 3336 (1971).
3. D. L. Beveridge, M. Mezei, P. K. Mehrotra, F. T. Marchese, G. Ravi-Shanker, T. Vasu, and S. Swaminathan, In *Molecular-Based Study of Fluids*, (*ACS Advances in Chemistry Series 204*), J. M. Haile and G. A. Mansoori, Eds., American Chemical Society, Washington, DC, 1983, p. 297.
4. (a) W. L. Jorgensen, J. Chandrasekhar, J. D. Madura, R. W. Impey, and M. L. Klein, *J. Chem. Phys.*, **79**, 926 (1983); (b) W. L. Jorgensen and J. D. Madura, *Mol. Phys.*, **56**, 1381 (1985).
5. H. J. C. Berendsen, J. P. M. Postma, W. F. van Gunsteren, and J. Hermans, In *Intermolecular Forces*, B. Pullman, Ed., Reidel, Dordrecht, 1981, p. 331.
6. F. H. Stillinger and A. Rahman, *J. Chem. Phys.*, **60**, 1545 (1974).
7. W. L. Jorgensen, *J. Am. Chem. Soc.*, **103**, 335 (1981).
8. See, for example: (a) M. Sprik and M. L. Klein, *J. Chem. Phys.*, **89**, 7556 (1988); (b) J. Caldwell, L. X. Dang, and P. A. Kollman, *J. Am. Chem. Soc.*, **112**, 9144 (1990); (c) S. Kuwajima and A. Warshel, *J. Phys. Chem.*, **94**, 460 (1990); (d) T. P. Straatsma and J. A. McCammon, *Chem. Phys. Lett.*, **177**, 433 (1991); D. van Belle and S. J. Wodak, *J. Am. Chem. Soc.*, **115**, 647 (1993); (f) S. W. Rick, S. J. Stuart, and B. J. Berne, *J. Chem. Phys.*, **101**, 6141 (1994).
9. (a) P. H. Poole, F. Sciortino, U. Essmann, and H. E. Stanley, *Phys. Rev. E*, **48**, 3799 (1993); (b) F. Sciortino, P. H. Poole, U. Essmann, and H. E. Stanley, *Phys. Rev. E*, **55**, 727 (1997); (c) H. Tanaka, *Nature*, **380**, 328 (1996); (d) H. Tanaka, *J. Chem. Phys.*, **105**, 5099 (1996).
10. (a) S. R. Billeter, P. M. King, and W. F. van Gunsteren, *J. Chem. Phys.*, **100**, 6692 (1994); (b) L. A. Báez and P. Clancy, *J. Chem. Phys.* **101**, 9837 (1994); (c) A. Wallqvist and P.-O. Åstrand, *J. Chem. Phys.*, **102**, 6559 (1995); (d) C. H. Cho, S. Singh, and G. W. Robinson, *Phys. Rev. Lett.*, **76**, 1651 (1996).
11. All calculations were performed with the BOSS program: W. L. Jorgensen, *BOSS*, *Version 3.8*, Yale University, New Haven, CT, 1996. The long runs were facilitated by execution on a cluster of personal computers with 200-MHz Pentium Pro processors running Linux; see J. Tirado-Rives and W. L. Jorgensen, *J. Comput. Chem.*, **17**, 1385 (1996). Roughly 60×10^6 Monte Carlo configurations could be run per day on each processor.
12. M. P. Allen and D. J. Tildesley, *Computer Simulations of Liquids*, Clarendon, Oxford, 1987.
13. W. L. Jorgensen, *Chem. Phys. Lett.*, **92**, 405 (1982).
14. (a) G. S. Kell, *J. Chem. Eng. Data*, **20**, 97 (1975); (b) N. E. Dorsey, *Properties of Ordinary Water Substance*, Reinhold, New York, 1940; (c) C. A. Angell, M. Oguni, and W. J. Sichina, *J. Chem. Phys.*, **86**, 998 (1982).
15. (a) H. E. Alper and R. M. Levy, *J. Chem. Phys.*, **91**, 1242 (1989); (b) P. E. Smith and W. F. van Gunsteren, *J. Chem. Phys.*, **100**, 3169 (1994).
16. K. Watanabe and M. L. Klein, *Chem. Phys.*, **131**, 157 (1989).
17. M. Ferrario and A. Tani, *Chem. Phys. Lett.*, **121**, 182 (1985).
18. M. Neumann, *J. Chem. Phys.*, **85**, 1567 (1986).
19. (a) H. J. C. Berendsen, J. R. Grigera, and T. P. Straatsma, *J. Phys. Chem.*, **91**, 6269 (1987); (b) M. R. Reddy and M. Berkowitz, *Chem. Phys. Lett.*, **155**, 173 (1991).
20. J. D. Madura, B. M. Pettitt, and D. F. Calef, *Mol. Phys.*, **64**, 325 (1988).
21. A. K. Soper and M. G. Phillips, *Chem. Phys.*, **107**, 47 (1985).
22. P. H. Poole, F. Sciortino, U. Essmann, and H. E. Stanley, *Nature*, **360**, 324 (1992).
23. For summaries, see: T. I. Mizan, P. E. Savage, and R. M. Ziff, *J. Phys. Chem.*, **98**, 13067 (1994); J. Gao, *J. Am. Chem. Soc.*, **115**, 6893 (1993).